Modelling the inactivation of viruses from the Coronaviridae family in response to temperature and relative humidity in suspensions or surfaces.

Laurent Guillier, Sandra Martin-Latil, Estelle Chaix, Anne Thébault, Nicole Pavio, Sophie Le Poder, Christophe Batéjat, Fabrice Biot, Lionel Koch, Don Schaffner, et al.

Modelling the inactivation of viruses from the *Coronaviridae* family in response to temperature and relative humidity in suspensions or surfaces.

Authors:

Laurent Guillier,[a] Sandra Martin-Latil,[b] Estelle Chaix,[a] Anne Thébault,[a] Nicole Pavio,[c] Sophie Le Poder,[c] on behalf of Covid-19 Emergency Collective Expert Appraisal Group,[d] Christophe Batéjat,[e] Fabrice Biot,[f], Lionel Koch,[f] Don Schaffner,[g] Moez Sanaa,[a]

Affiliations:

[a]Risk Assessment Department, French Agency for Food, Environmental and Occupational Health & Safety, 14, rue Pierre et Marie Curie, Maisons-Alfort, France

[b]Laboratory for food safety French Agency for Food, Environmental and Occupational Health & Safety, University of Paris-EST, Maisons-Alfort, France

[c]UMR Virologie 1161, ENVA, INRAE, Anses, Maisons-Alfort, France

[d]Membership of the Covid-19 Emergency Collective Expert Appraisal Group is provided in the Acknowledgments

[e]Environment and Infectious Risks Unit, Laboratory for Urgent Response to Biological Threats (CIBU), Institut Pasteur, Paris, France

[f]Bacteriology Unit, French Armed Forces Biomedical Research Institute (IRBA), Brétigny-sur-Orge, France

[g]Department of Food Science, Rutgers University, New Brunswick, NJ, USA

Affiliations:

Running Head: Modelling the inactivation of coronaviruses on fomites

#Address correspondence to laurent.guillier@anses.fr

Abstract:

Temperature and relative humidity are major factors determining virus inactivation in the environment. This article reviews inactivation data of coronaviruses on surfaces and in liquids from published studies and develops secondary models to predict coronaviruses inactivation as a function of temperature and relative humidity. A total of 102 D-values (time to obtain a $\log_{10}$ reduction of virus infectivity), including values for SARS-CoV-2, were collected from 26 published studies. The values obtained from the different coronaviruses and studies were found to be generally consistent. Five different models were fitted to the global dataset of D-values. The most appropriate model considered temperature and relative humidity. A spreadsheet predicting the inactivation of coronaviruses and the associated uncertainty is presented and can be used to predict virus inactivation for untested temperatures, time points or any coronavirus strains belonging to *Alphacoronavirus* and *Betacoronavirus* genera.

Importance: The prediction of the persistence of SARS-CoV-2 on fomites is essential to investigate the importance of contact transmission. This study collects available information on inactivation kinetics of coronaviruses in both solid and liquid fomites and creates a mathematical model for the impact of temperature and relative humidity on virus persistence. The predictions of the model can support more robust decision-making and could be useful in various public health contexts. Having a calculator for the natural clearance of SARS-CoV-2 depending on temperature and relative humidity could be a valuable operational tool for public authorities.

Keywords: Persistence, coronavirus, modelling, fomites, SARS-CoV-2

1. Introduction

The pandemic of coronavirus respiratory infectious disease (COVID-19) initiated in Wuhan, China in December 2019 was caused by an emergent virus named Severe Acute Respiratory Syndrome Coronavirus 2 (SARS-CoV-2). SARS-CoV-2 belongs to the order *Nidovirales*, family *Coronaviridae*. These enveloped viruses have a positive, single-stranded RNA genome (directly translated) surrounded by a nucleocapsid protein. Coronaviruses are classified into four genera: alpha (αCoV), beta (βCoV), gamma (ɣCoV), and delta (δCoV). SARS-CoV-2 belongs to the *Betacoronavirus* genus and the *Sarbecovirus* sub-genus.

The route of transmission of respiratory viruses is airborne via inhalation of droplets and aerosols or through contact with contaminated intermediate objects (fomites), e.g. by self-inoculation of mucous membranes (mouth, eyes) by contaminated hands (1). The transmission route for SARS-CoV-2, SARS-CoV and Middle East respiratory syndrome (MERS-CoV) is primarily airborne (2-5) while environmental contamination through surfaces is uncertain (6-8). No study has currently quantified the importance of surface contact transmission in the spread of coronavirus diseases (9). Viral genomes have been detected in the stools of COVID-19 patients and sewage (10), but the role of liquid fomites has not yet been addressed.

Working with highly virulent coronavirus requires biosafety level 3 laboratory containment conditions and since SARS-CoV2 emerged very recently, few data on its survival related to environmental conditions are available (11, 12). The use of surrogate coronaviruses has been suggested to overcome these challenges and expand the available data on coronavirus survival likelihood (13). Surrogates can be used under the

assumption that they have similar physicochemical properties that mimic the viruses they represent (14, 15).

Temperature and relative humidity have been shown to impact the kinetics of inactivation of coronaviruses. Increased temperatures have been shown to increase the rate of the inactivation (11, 16), and decreased relative humidity have been associated with a reduction of coronaviruses inactivation rate on surfaces (13, 17-19). Inactivation rates were lower in suspensions compared to surfaces in studies that tested both suspensions and surfaces at similar temperatures (11, 20).

Hence, the prediction of the persistence of SARS-CoV-2 on fomites is essential to investigate the importance of contact transmission. This study collects available information on inactivation kinetics of coronaviruses in both solid and liquid fomites and models the impact of temperature and relative humidity on virus persistence.

2. Materials & methods

2.1. Selection of the studies

Four inclusion criteria were used to identify studies that characterized inactivation of coronaviruses according to temperature and relative humidity. Selected studies had to focus on one virus from the *Coronaviridae* family. Inactivation must have been carried out in suspensions or on inert non-porous surfaces. Only surfaces without antimicrobial properties were considered. The quantification of infectious viruses had to be assessed by cell culture, since RT-qPCR can underestimate actual virus infectivity (21, 22). Finally, the available kinetics data points should be sufficient to allow precise statistical estimation of the rate of viral inactivation without bias. In this context, kinetic data with

no significant inactivation observed during the experiment or with values below the quantification limit in the first time interval were not included.

2.2. Data collection

The kinetics were gathered from either the figures or the tables of the selected studies. The digitize R package (23) was used to retrieve data from scatter plots in figures. This package loads a graphical file of a scatterplot (in jpeg format) in the graphical window of R and calibrates and extracts the data. Data were manually reported in R vector for data provided in tables. A key was attributed to kinetics collected in each study (Table 1). The specific list of tables and figures used for each kinetics is given in appendix 1.

2.3. Modelling of inactivation

A simple primary model was used for describing each inactivation kinetics. The D-values (or decimal reduction times) were determined from the kinetics of the $\log_{10}$ number of infectious viruses (*N*) over time at each experimental temperature. *D* is the inverse of the slope of the inactivation kinetics.

$$log_{10}(N) = log_{10}(N_0) - {}^{t}/_{D} \qquad \text{eq. (1)}$$

Several secondary models describing the impact of temperature (T) and relative humidity (RH) on *D* values were tested. The gamma concept of inactivation was used (24, 25). In this approach, the inactivation of a microbial population could be estimated by:

$$log_{10}(D) = log_{10}\left(D_{ref}\right) - \sum log_{10}\left(\lambda_{xi}(x_i)\right) \qquad \text{eq. (2)}$$

Where λ_{xi} quantifies the influence of each environmental factors (x_i corresponds to temperature and relative humidity in this study) on the microbial resistance (D_{ref}) observed in reference conditions.

Based on eq. (2), five different secondary models were established. Models #1, #2 and #3 do not consider the nature of the fomite.

Model #1 is the classical Bigelow model (26). It models only the effect of temperature. The z_T, the increase of temperature which leads to a tenfold reduction of D, value was determined as the negative inverse slope of the plot of $\log_{10}(D)$ versus temperature. z_T is the increase of temperature which leads to a ten-fold reduction of the decimal reduction time. T_{ref} is the reference temperature (set to 4°C in our study) and $\log_{10}(D_{ref})$ is the $\log_{10}(D)$ at T_{ref}.

Model #1

$log_{10}(\lambda_T(T)) = \frac{T-T_{ref}}{z}$ and $log_{10}(\lambda_{RH}(RH)) = 0$

Model #2 considers the effect of temperature, however D values were fitted according to temperature using a semi-log approach, derived from Mafart (25).

$log_{10}(\lambda_T(T)) = \left(\frac{T-T_{ref}}{Z_T}\right)^2$ and $log_{10}(\lambda_{RH}(RH)) = 0$

Model #3 is similar to model #2 but the shape parameter n was estimated instead of being set to 2.

$log_{10}(\lambda_T(T)) = \left(\frac{T-T_{ref}}{Z_T}\right)^n$ and $log_{10}(\lambda_{RH}(RH)) = 0$

The last two models (#4 and #5) consider the effect of temperature and the nature of the fomites. The type of fomite was taken into account through the use of relative humidity. Suspensions correspond to more than 99% RH conditions while surfaces are associated with RH conditions below to this threshold. The models consider that surfaces at higher relative humidity allow for more rapid inactivation and that inactivation in suspensions is equivalent to inactivation on surfaces exposed to low RH. In model #4, the shape parameter for temperature was set to 2 as in model #2.

$log_{10}(\lambda_T(T)) = \left(\frac{T-T_{ref}}{Z_T}\right)^2$ and $log_{10}(\lambda_{RH}(RH)) = \begin{cases} \frac{\mathrm{RH}}{z_{RH}} & RH < 99\% \\ 0 & RH \geq 99\% \end{cases}$

In model #5, n is a model parameter to be estimated.

$log_{10}(\lambda_T(T)) = \left(\frac{T-T_{ref}}{Z_T}\right)^n$ and $log_{10}(\lambda_{RH}(RH)) = \begin{cases} \frac{\mathrm{RH}}{z_{RH}} & RH < 99\% \\ 0 & RH \geq 99\% \end{cases}$

In models #4 and #5, z_{RH} is the increase of relative humidity, which leads to a ten-fold reduction of the decimal reduction time.

2.4. Model's parameters estimation

The model's parameters were fitted with nls() R function. Confidence intervals of fitted parameters were assessed by bootstrap using nlsBoot() function from nlsMicrobio R package (27). The five models were compared according to penalized-likelihood criteria, the Aikaike information criterion (AIC) (28) and Bayesian information criterion (BIC) (29).

$$AIC = p.Ln\left(\frac{RSS}{p}\right) + 2k$$

$$BIC = p.Ln\left(\frac{RSS}{p}\right) + k.Ln(p)$$

Where RSS is the residual sum of squares, p is the number of experimental points and k the number of parameters in the model. The lower the AIC and BIC, the better the model fits the dataset.

2.5. Data availability

The detailed information on the tables and figures where the data were collected are given in appendix 1. All the scripts and data used to prepare figures and tables of this manuscript are available in a Github repository (30).

3. Results

3.1. Literature review results

Table 1 shows the detailed characteristics of the twenty-six studies that characterized inactivation of a virus from the *Coronaviridae* family according to temperature and or relative humidity. Some kinetics were not appropriate for characterizing inactivation rate either because the duration of the experiments was too short to observe any significant decrease of virus infectivity, or because the quantification limit was reached before the first time point (Table 1). A total of 102 estimates of D-value were collected from 25 of the 26 studies (Appendix 1). These kinetic values represent 605 individual data points. For each curve, a D-value (i.e. decimal reduction time) was estimated. The 102 D-values are given in Appendix 1. Among the 102 kinetic values, 44 are from members of the *Alphacoronavirus* genus including one from Canine coronavirus (CCV), two for the feline infectious peritonitis virus (FIPV), five for the porcine epidemic diarrhea virus (PEDV), 14 for the Human coronavirus 229E (HCoV-229E) and 22 from the porcine transmissible gastroenteritis coronavirus (TGEV). The remaining 58 kinetics are related to the

175 *Betacoronavirus* genus, including two Human coronavirus - OC43 (HCoV-OC43), two for
176 the bovine coronavirus, 13 for the murine hepatitis virus (MHV), eight for the MERS-
177 CoV, 22 for the SARS-CoV and 11 for the SARS-CoV-2. Figure 1 shows the 102
178 estimates of D-values, including 40 values on inert surfaces and 62 values in
179 suspension from temperatures ranging from 4°C to 68°C. Different suspensions were
180 noted, but most were laboratory media (Table 1).

181 **3.2. Modelling the inactivation**

182 The 102 D-values were fitted with five different models. Table 2 shows the performance
183 of these models to describe D-values according to temperature and relative humidity.
184 For the tested range of temperatures (between 4 and 68°C), model #1 (the classical
185 Bigelow model) based on a log-linear relation between D-values and temperature does
186 not perform as well as model #2 that considers a linear second-degree equation. Model
187 #3 offers a further refinement over model #2 by also fitting the degree of the equation (*n*
188 parameter). The fitted value of *n* was equal to 1.9 with a confidence interval that
189 includes 2 (*i.e.* model #2). Accordingly, the values taken by the parsimony criterions for
190 model selection AIC and BIC for model #2 and #3, indicate that *n* can be set to 2.

191 Figure 2 illustrates the performance of models #1 (Fig. 2A), #2 (Fig. 2B) and #3 (Fig. 3C)
192 for which only temperature effect is considered for predicting D-values.

193 Table 2 demonstrates that the inclusion of relative humidity should be considered.
194 Models #4 and #5 that describe the D-values according to temperature and relative
195 humidity were more appropriate models than models #1, #2 and #3 with a decrease of
196 AIC of more than 2 points in comparison with other models (31). The estimated value for
197 the shape parameter in model #5 is not different from the value two. According to BIC

198 criterion, model #4 and model #2 were the most appropriate and undistinguishable.
199 Based on these comparisons, model #4 was retained. Figure 3A shows the prediction of
200 inactivation rate according to T and RH for this model. The high z_{RH} value (Table 2)
201 indicates that the impact of RH is far less important than temperature. For example,
202 increasing the relative humidity by 80%, e.g. from 10% to 90%, only reduces the D
203 values by a factor of 1.7. The same reduction factor of D-values can be obtained by a
204 small change of temperature, (e.g. changing from 10 to 15°C or from 60 to 61°C). Model
205 #2 was retained as well as it provides very similar performance. Figures 3B shows the
206 residuals for model #4. Comparative analysis of residuals of models #2 and #4 are
207 provided in Appendix 2 (Figure A2-1).
208
209 **3.3. Potential use of the model**
210 An Excel spreadsheet implementing model #4 has been prepared and is available in
211 Appendix 3. The spreadsheet can be used to estimate the number of decimal reductions
212 of infectivity of coronaviruses according to user defined time, temperature and relative
213 humidity. For example, the predicted inactivation at a temperature of 70°C for 1 minute
214 in liquid is -11.8 $\log_{10}$ with a 95% CI [-6.4; -22.1] for model #4 and -11.1 $\log_{10}$ with a
215 95% CI [-5.7; -21.4] for model #2. The spreadsheet also allows an estimate of the time
216 necessary to reach a target number of decimal reductions of infectivity with a certain
217 confidence level for both model #4 and model #2. For example, the time to reach a 5
218 $\log_{10}$ inactivation at 20°C and 75% relative humidity is 304 h with a 95% CI of [215; 426].
219 It will be much longer at 20% relative humidity as the time to reach a 5 $\log_{10}$ inactivation
220 is predicted to be 438 h with a 95% CI of [339; 569]. Model #2 (that does not take into

account relative humidity), provides an estimate of the time to reach a 5 $\log_{10}$ inactivation at 20°C of 412 h with a 95% CI of [322; 539].

4. Discussion

Our study identified 102 kinetic values for inactivation of coronaviruses on surfaces and in suspensions. The included studies cover those identified in three recently published articles that conducted a systematic review on coronaviruses inactivation (32-34). These data were used to suggest a novel inactivation model specific to the *Coronaviridae* family. The modelling approach identified temperature and relative humidity as major factors needed to predict infectious coronavirus persistence on fomites.

The $\log_{10}$ of D values was not linearly related to temperature in the range of temperatures studied (4 – 68°C). Bertrand et al. (15) made a similar observation in a meta-analysis for virus and phage inactivation in foods and water and proposed two different models on either side of the threshold temperature of 50°C. Laude (16) suggested a similar approach for TGEV with a threshold temperature at 45°C (16). The modelling approach we used in our study allows fitting the inactivation values with a single relation. In other meta-analysis on inactivation of viruses, Boehm et al. (22) and Heßling et al. (35) did not observe such different trends but also studied smaller temperature ranges. In the highest range of temperature (above 60°C), coronaviruses are found to be far less heat resistant than non-enveloped viruses (36).

The present modelling approach considers the non-monotonous impact of relative humidity on inactivation. Coronaviruses persisted better at low RHs and at 100% RH, than for intermediate RHs. Another study has confirmed that low RH makes viruses

more resistant to thermal inactivation (37). Lin and Marr (38) recently observed the same relation for two bacteriophages, where the observed RH where survival was worst is close to 80% while in the present study, the less favorable condition for coronaviruses was set to 99%. The data collected in the present study do not cover a uniform distribution of temperatures and RH values. Further data corresponding to inactivation of coronaviruses on surfaces at low humidities for temperature between 40 and 60°C would help to refine assessment of impact of RH. Using a worst-case RH set to 99% may be appropriate to estimate reductions in those situations until the model can be refined.

As noted in the methods, all the kinetic values analyzed were established based on the quantification of coronavirus infectivity with cell cultures. The model prediction did not include other inactivation results from methods combining dyes with RT-qPCR. This method (although more appropriate than classical RT-qPCR) can underestimate virus infectivity (21, 22).

The data collected from the literature does not permit models specific to species at this time. Our findings suggest that persistence potential of different coronaviruses is similar. It confirms previous finding that advocates for the use of surrogates' coronavirus such as TGEV (39). This could considerably simplify the acquisition of relevant data for persistence potential for other environmental factors. The data analyzed here only include *Alpha*- and *Betacoronavirus*, as no data for the two other major genera, *Delta*- and *Gammacoronavirus*, were identified. Inclusion of such data would help to challenge the present model robustness.

The models developed in our study are specific to viruses from the *Coronaviridae* family. Several studies on the inactivation of other viruses have suggested that the impact of

268 temperature can be modelled, as a whole, with a unique parameter (15, 22, 40).
269 Variability of behavior by virus type has been observed and model parameters to
270 account these differences have been proposed (22, 40), e.g. non-enveloped viruses are
271 known to show greater persistence in the environment (40). Like a recently proposed
272 model for SARS-CoV-2 (41), our model takes into consideration of relative humidity in
273 the prediction of inactivation. This integration is of high interest in the perspective of
274 assessment of seasonality on virus persistence (42).
275 It's also worth noting our model is specific to fomites. Survival kinetics in fecal materials
276 were identified (43) but not considered for inclusion. The level of matrix contamination
277 with fecal materials has been shown to significantly increase the inactivation rate of
278 viruses (40), so by excluding these data, model predictions are biased to be fail-safe.
279 Inactivation data on porous surfaces were also not considered since it may be difficult to
280 determine if any measured inactivation is associated with real loss of infectivity or
281 difficulty in recovering viruses absorbed inside the porous material. That said, there is no
282 reason to consider that model predictions for coronaviruses are not pertinent to survival
283 on porous material (e.g. face masks).
284 Inactivation on anti-microbial surfaces, such as copper and silver, was also not
285 considered. For the same reason, model predictions are fail safe as surfaces including
286 copper or other antimicrobial compounds increase the inactivation rate of coronaviruses
287 (12, 44).
288 The predictions of the present model could support more robust decision-making and
289 could be useful in various contexts such as blood safety assessment (45) or validation of
290 thermal inactivating treatments for room air, surfaces or suspensions. Indeed, an
291 important issue is the possibility of reusing privates or public offices, rooms of hotels, or

vehicles that are difficult to decontaminate. Moreover, many devices like electronics or more sensitive materials, are not suitable for chemical decontamination processes which could make them inoperative. Another aspect of decontamination is the economical challenge as large scale decontamination of buildings can cost billions of dollars (46). Furthermore, the use of detergents and/or disinfectants may have environmental consequences. Thus the large scale decontamination of surfaces for SARS-CoV-2 that are not necessarily in contact with people may not be required. For these reasons the waiting time needed before handling suspected contaminated materials in absence of decontamination is more than ever an important question. Having a calculator for the natural clearance of SARS-CoV-2 depending on temperature could be a valuable operational tool for public authorities (41).

The present model also opens the way for risk assessment for SARS-CoV-2 transmission through contact (47). Further model developments including data on matrix pH, salinity and exposure to visible and UV light would also be important to consider (40, 48).

5. Acknowledgements

The Covid-19 Emergency Collective Expert Appraisal Group members included the co-authors LG, S.M-L, E.C, N.P, S.L.P, M.S. and (in alphabetical order): Paul Brown, Charlotte Dunoyer, Florence Etore, Elissa Khamisse, Meriadeg Legouil, François Meurens, Gilles Meyer, Elodie Monchatre-Leroy, Gaëlle Simon and Astrid Vabret.

6. References

1. Kutter JS, Spronken MI, Fraaij PL, Fouchier RA, Herfst S. 2018. Transmission routes of respiratory viruses among humans. Current Opinion in Virology 28:142-151.
2. Lu J, Gu J, Li K, Xu C, Su W, Lai Z, Zhou D, Yu C, Xu B, Yang Z. 2020. COVID-19 Outbreak associated with air conditioning in restaurant, Guangzhou, China, 2020. Emerging Infectious Diseases 26.
3. Lee N, Hui D, Wu A, Chan P, Cameron P, Joynt GM, Ahuja A, Yung MY, Leung C, To K. 2003. A major outbreak of severe acute respiratory syndrome in Hong Kong. New England Journal of Medicine 348:1986-1994.
4. Kim S-H, Chang SY, Sung M, Park JH, Bin Kim H, Lee H, Choi J-P, Choi WS, Min J-Y. 2016. Extensive viable Middle East respiratory syndrome (MERS) coronavirus contamination in air and surrounding environment in MERS isolation wards. Reviews of Infectious Diseases 63:363-369.
5. Liu J, Liao X, Qian S, Yuan J, Wang F, Liu Y, Wang Z, Wang F, Liu L, Zhang Z. 2020. Community transmission of Severe Acute Respiratory Syndrome Coronavirus 2, Shenzhen, China, 2020. Emerging Infectious Diseases 26.
6. Chen Y-C, Huang L-M, Chan C-C, Su C-P, Chang S-C, Chang Y-Y, Chen M-L, Hung C-C, Chen W-J, Lin F-Y. 2004. SARS in hospital emergency room. Emerging Infectious Diseases 10:782.
7. Danis K, Epaulard O, Bénet T, Gaymard A, Campoy S, Bothelo-Nevers E, Bouscambert-Duchamp M, Spaccaferri G, Ader F, Mailles A, Boudalaa Z, Tolsma V, Berra J, Vaux S, Forestier E, Landelle C, Fougere E, Thabuis A, Berthelot P, Veil R, Levy-Bruhl D, Chidiac C, Lina B, Coignard B, Saura C, Team I. 2020. Cluster of coronavirus disease 2019 (Covid-19) in the French Alps, 2020. Clinical Infectious Diseases doi:10.1093/cid/ciaa424.
8. Otter JA, Donskey C, Yezli S, Douthwaite S, Goldenberg SD, Weber DJ. 2016. Transmission of SARS and MERS coronaviruses and influenza virus in healthcare settings: the possible role of dry surface contamination. Journal of Hospital Infection 92:235-250.
9. Wolff MH, Sattar SA, Adegbunrin O, Tetro J. 2005. Environmental survival and microbicide inactivation of coronaviruses, p 201-212, Coronaviruses with special emphasis on first insights concerning SARS. Springer.
10. Medema G, Heijnen L, Elsinga G, Italiaander R, Brouwer A. 2020. Presence of SARS-Coronavirus-2 in sewage. medRxiv doi:https://doi.org/10.1101/2020.03.29.20045880.
11. Chin A, Chu J, Perera M, Hui K, Yen H-L, Chan M, Peiris M, Poon L. 2020. Stability of SARS-CoV-2 in different environmental conditions. . The Lancet Microbe https://doi.org/10.1016/S2666-5247(20)30003-3.
12. van Doremalen N, Bushmaker T, Morris DH, Holbrook MG, Gamble A, Williamson BN, Tamin A, Harcourt JL, Thornburg NJ, Gerber SI. 2020. Aerosol and surface stability of SARS-CoV-2 as compared with SARS-CoV-1. New England Journal of Medicine.
13. Casanova LM, Jeon S, Rutala WA, Weber DJ, Sobsey MD. 2010. Effects of air temperature and relative humidity on coronavirus survival on surfaces. Appl Environ Microbiol 76:2712-2717.

14. Bozkurt H, D'Souza DH, Davidson PM. 2015. Thermal inactivation kinetics of human norovirus surrogates and hepatitis A virus in turkey deli meat. Appl Environ Microbiol 81:4850-4859.
15. Bertrand I, Schijven J, Sánchez G, Wyn-Jones P, Ottoson J, Morin T, Muscillo M, Verani M, Nasser A, de Roda Husman A. 2012. The impact of temperature on the inactivation of enteric viruses in food and water: a review. Journal of Applied Microbiology 112:1059-1074.
16. Laude H. 1981. Thermal inactivation studies of a coronavirus, transmissible gastroenteritis virus. Journal of General Virology 56:235-240.
17. Van Doremalen N, Bushmaker T, Munster V. 2013. Stability of Middle East respiratory syndrome coronavirus (MERS-CoV) under different environmental conditions. Eurosurveillance 18:20590.
18. Ijaz M, Brunner A, Sattar S, Nair RC, Johnson-Lussenburg C. 1985. Survival characteristics of airborne human coronavirus 229E. Journal of General Virology 66:2743-2748.
19. Ijaz M, Karim Y, Sattar S, Johnson-Lussenburg C. 1987. Development of methods to study the survival of airborne viruses. Journal of Virological Methods 18:87-106.
20. Rabenau H, Cinatl J, Morgenstern B, Bauer G, Preiser W, Doerr H. 2005. Stability and inactivation of SARS coronavirus. Medical Microbiology and Immunology 194:1-6.
21. Coudray-Meunier C, Fraisse A, Martin-Latil S, Guillier L, Perelle S. 2013. Discrimination of infectious hepatitis A virus and rotavirus by combining dyes and surfactants with RT-qPCR. BMC microbiology 13:216.
22. Boehm AB, Silverman AI, Schriewer A, Goodwin K. 2019. Systematic review and meta-analysis of decay rates of waterborne mammalian viruses and coliphages in surface waters. Water research 164:114898.
23. Poisot T. 2011. The digitize package: extracting numerical data from scatterplots. The R Journal 3:25-26.
24. Coroller L, Kan-King-Yu D, Leguerinel I, Mafart P, Membré J-M. 2012. Modelling of growth, growth/no-growth interface and nonthermal inactivation areas of *Listeria* in foods. International Journal of Food Microbiology 152:139-152.
25. Mafart P. 2000. Taking injuries of surviving bacteria into account for optimising heat treatments. International Journal of Food Microbiology 55:175-179.
26. Bigelow W. 1921. The logarithmic nature of thermal death time curves. The Journal of Infectious Diseases:528-536.
27. Baty F, Delignette-Muller M. 2017. nlsMicrobio: data sets and nonlinear regression models dedicated to predictive microbiology. R package version 0.0-1.
28. Akaike H. 1974. A new look at the statistical model identification. IEEE Transactions on Automatic Control 19:716-723.
29. Schwarz G. 1978. Estimating the dimension of a model. The Annals of Statistics 6:461-464.
30. Guillier L. 2020. Data and models related to coronaviruses inactivation. https://github.com/lguillier/Persistence-Coronavirus.
31. Burnham KP, Anderson DR. 1998. Practical use of the information-theoretic approach, p 75-117, Model selection and inference. Springer.

32. Kampf G, Voss A, Scheithauer S. 2020. Inactivation of coronaviruses by heat. Journal of Hospital Infection.
33. La Rosa G, Bonadonna L, Lucentini L, Kenmoe S, Suffredini E. 2020. Coronavirus in water environments: Occurrence, persistence and concentration methods-A scoping review. Water Research:115899.
34. Kampf G, Todt D, Pfaender S, Steinmann E. 2020. Persistence of coronaviruses on inanimate surfaces and its inactivation with biocidal agents. Journal of Hospital Infection.
35. Heßling M, Hoenes K, Lingenfelder C. 2020. Selection of parameters for thermal Coronavirus inactivation–A data-based recommendation. GMS Hygiene and Infection Control in press.
36. Firquet S, Beaujard S, Lobert P-E, Sané F, Caloone D, Izard D, Hober D. 2014. Viruses contained in droplets applied on warmed surface are rapidly inactivated. Microbes and Environments 29:408-412.
37. Sauerbrei A, Wutzler P. 2009. Testing thermal resistance of viruses. Archives of virology 154:115-119.
38. Lin K, Marr LC. 2019. Humidity-Dependent Decay of Viruses, but Not Bacteria, in Aerosols and Droplets Follows Disinfection Kinetics. Environmental Science & Technology 54:1024-1032.
39. Casanova L, Rutala WA, Weber DJ, Sobsey MD. 2009. Survival of surrogate coronaviruses in water. Water research 43:1893-1898.
40. Brainard J, Pond K, Hunter PR. 2017. Censored regression modeling to predict virus inactivation in wastewaters. Environmental science & technology 51:1795-1801.
41. United States Department of Homeland Security. 2020. SARS-CoV-2 Indoor Environmental Stability Predictive Model. Available at: https://www.dhs.gov/sites/default/files/publications/sars-cov-2_environment_predictive_model_factsheet_2.pdf
42. Prussin AJ, Schwake DO, Lin K, Gallagher DL, Buttling L, Marr LC. 2018. Survival of the enveloped virus Phi6 in droplets as a function of relative humidity, absolute humidity, and temperature. Appl Environ Microbiol 84:e00551-18.
43. Lai MY, Cheng PK, Lim WW. 2005. Survival of severe acute respiratory syndrome coronavirus. Clinical Infectious Diseases 41:e67-e71.
44. Warnes SL, Little ZR, Keevil CW. 2015. Human coronavirus 229E remains infectious on common touch surface materials. MBio 6:e01697-15.
45. Chang L, Yan Y, Wang L. 2020. Coronavirus Disease 2019: Coronaviruses and Blood Safety. Transfusion Medicine Reviews doi:https://doi.org/10.1016/j.tmrv.2020.02.003.
46. Schmitt K, Zacchia NA. 2012. Total decontamination cost of the anthrax letter attacks. Biosecurity and bioterrorism: biodefense strategy, practice, and science 10:98-107.
47. Haas C. 2020. Coronavirus and Risk Analysis. Risk Analysis 40:660-661.
48. Heßling M, Hönes K, Vatter P, Lingenfelder C. 2020. Ultraviolet irradiation doses for coronavirus inactivation–review and analysis of coronavirus photoinactivation studies. GMS Hygiene and Infection Control 15.

49. Mullis L, Saif LJ, Zhang Y, Zhang X, Azevedo MS. 2012. Stability of bovine coronavirus on lettuce surfaces under household refrigeration conditions. Food Microbiology 30:180-186.
50. Saknimit M, Inatsuki I, Sugiyama Y, Yagami K. 1988. Virucidal efficacy of physico-chemical treatments against coronaviruses and parvoviruses of laboratory animals. Jikken dobutsu Experimental animals 37:341.
51. Christianson K, Ingersoll J, Landon R, Pfeiffer N, Gerber J. 1989. Characterization of a temperature sensitive feline infectious peritonitis coronavirus. Archives of Virology 109:185-196.
52. Gundy PM, Gerba CP, Pepper IL. 2009. Survival of coronaviruses in water and wastewater. Food and Environmental Virology 1:10.
53. Bucknall RA, King LM, Kapikian AZ, Chanock RM. 1972. Studies with human coronaviruses II. Some properties of strains 229E and OC43. Proceedings of the Society for Experimental Biology and Medicine 139:722-727.
54. Sizun J, Yu M, Talbot P. 2000. Survival of human coronaviruses 229E and OC43 in suspension and after drying onsurfaces: a possible source ofhospital-acquired infections. Journal of Hospital Infection 46:55-60.
55. Lamarre A, Talbot PJ. 1989. Effect of pH and temperature on the infectivity of human coronavirus 229E. Canadian Journal of Microbiology 35:972-974.
56. Leclercq I, Batejat C, Burguière AM, Manuguerra JC. 2014. Heat inactivation of the Middle East Respiratory Syndrome coronavirus. Influenza and Other Respiratory Viruses 8:585-586.
57. Ye Y, Ellenberg RM, Graham KE, Wigginton KR. 2016. Survivability, partitioning, and recovery of enveloped viruses in untreated municipal wastewater. Environmental Science & Technology 50:5077-5085.
58. Hofmann M, Wyler R. 1989. Quantitation, biological and physicochemical properties of cell culture-adapted porcine epidemic diarrhea coronavirus (PEDV). Veterinary Microbiology 20:131-142.
59. Quist-Rybachuk G, Nauwynck H, Kalmar I. 2015. Sensitivity of porcine epidemic diarrhea virus (PEDV) to pH and heat treatment in the presence or absence of porcine plasma. Veterinary microbiology 181:283-288.
60. Hulst MM, Heres L, Hakze-van der Honing R, Pelser M, Fox M, van der Poel WH. 2019. Study on inactivation of porcine epidemic diarrhoea virus, porcine sapelovirus 1 and adenovirus in the production and storage of laboratory spray-dried porcine plasma. Journal of Applied Microbiology 126:1931-1943.
61. Darnell ME, Subbarao K, Feinstone SM, Taylor DR. 2004. Inactivation of the coronavirus that induces severe acute respiratory syndrome, SARS-CoV. Journal of virological methods 121:85-91.
62. Chan K, Peiris J, Lam S, Poon L, Yuen K, Seto W. 2011. The effects of temperature and relative humidity on the viability of the SARS coronavirus. Advances in Virology 2011.
63. Pagat A-M, Seux-Goepfert R, Lutsch C, Lecouturier V, Saluzzo J-F, Kusters IC. 2007. Evaluation of SARS-Coronavirus decontamination procedures. Applied Biosafety 12:100-108.
64. Kariwa H, Fujii N, Takashima I. 2006. Inactivation of SARS coronavirus by means of povidone-iodine, physical conditions and chemical reagents. Dermatology 212:119-123.

65. Batejat C, Grassin Q, Manuguerra J-C, Leclercq I. 2020. Heat inactivation of the Severe Acute Respiratory Syndrome Coronavirus 2. bioRxiv:https://doi.org/10.1101/2020.05.01.067769.

503 **Table 1. Characteristics of the studies that explored inactivation of infectivity of coronavirus.**

Virus	Genus	Sub-genus	Strain	Measurement	Temperatures (°C)	Conditions associated with treatment	Study reference
BCoV	*Betacoronavirus*	*Embecovirus*	Strain 88	PFU in Human rectal tumor (HRT)-18 cells	4	Salad, Minimal Essential Media (MEM) containing 2% Fetal Bovine Serum (FBS)	(49)
CCV	*Alphacoronavirus*	*Tegacovirus*	I-71	CRFK cells (PFU)	60, 80[a]	MEM containing 2% Fetal Calf Serum (FCS)	(50)
FIPV	*Alphacoronavirus*	*Tegacovirus*	DF2-WT	Feline kidney (NLFK) cells	54	Basal Medium Eagle	(51)
FIPV	*Alphacoronavirus*	*Tegacovirus*	ATCC-990	Crandell Reese feline kidney cell line	4[b], 23	Dechlorinated, filtered tap water	(52)
HCoV	*Alphacoronavirus*	*Duvinacovirus*	229E	Cellular infectivity in cell strain (HDCS) WI38	33, 37	Maintenance medium 2% FCS	(53)
HCoV	*Alphacoronavirus*	*Duvinacovirus*	229E	Cellular infectivity in lung cell line L132	21[b]	PBS, Earle's MEM, Earle's MEM to with added suspended cells	(54)
HCoV	*Alphacoronavirus*	*Duvinacovirus*	229E	Cellular infectivity in lung cell line L132	21[b]	Aluminum, sponge, latex at 65% RH	(54)
HCoV	*Alphacoronavirus*	*Duvinacovirus*	229E	CPE on MRC-5 cells	21	Teflon, PVC, Rubber, Steel, Plastic	(44)
HCoV	*Alphacoronavirus*	*Duvinacovirus*	229E	-	23	Cell culture supernatant with or without FBS	(20)
HCoV	*Alphacoronavirus*	*Duvinacovirus*	229E	MRC-5 cells (TCID-50)	4[b], 23	Dechlorinated, filtered tap water	(52)
HCoV	*Alphacoronavirus*	*Duvinacovirus*	229E	Cellular infectivity in lung cell line L132	4[b], 22, 33, 37	Earle's MEM	(55)
HCoV	*Betacoronavirus*	*Embecovirus*	OC43	Cellular infectivity in cell strain (HDCS) WI38	33, 37	Maintenance medium 2% FCS	(53)
HCoV	*Betacoronavirus*	*Embecovirus*	OC43	Cellular infectivity in human rectal tumor cell line HRT-18	21[b]	PBS, Earle's MEM, Earle's MEM to with added suspended cells	(54)
HCoV	*Betacoronavirus*	*Embecovirus*	OC43	Cellular infectivity in human rectal tumor cell line HRT-18	21[b]	Aluminum, sponge[a], latex[a] at 65% RH	(54)
MERS-	*Betacoronavirus*	*Sarbecovirus*	FRA2	Cellular infectivity in	25[b], 56, 65	Cell culture supernatant	(56)

CoV				Vero cells (TCID-50)			
MERS-CoV	*Betacoronavirus*	*Sarbecovirus*	HCoV-EMC/2012	Cellular infectivity in Vero cells (TCID-50)	20, 30	Plastic (30%, 40% or 80% RH)	(17)
MERS-CoV	*Betacoronavirus*	*Sarbecovirus*	HCoV-EMC/2012	Cellular infectivity in Vero cells (TCID-50)	20, 30	Plastic (30%, 40% or 80% RH)	(17)
MHV	*Betacoronavirus*	*Embecovirus*	-	Cellular infectivity in DBT cells	4[b], 25	Reagent-grade water	(39)
MHV	*Betacoronavirus*	*Embecovirus*	-	Cellular infectivity in DBT cells	4[b], 25	Lake water	(39)
MHV	*Betacoronavirus*	*Embecovirus*	-	Cellular infectivity in DBT cells	4[b], 20, 40	Stainless steel surface with 20% humidity	(13)
MHV	*Betacoronavirus*	*Embecovirus*	-	Cellular infectivity in DBT cells	4, 20, 40	Stainless steel surface with 50% humidity	(13)
MHV	*Betacoronavirus*	*Embecovirus*	-	Cellular infectivity in DBT cells	4, 20, 40	Stainless steel surface with 80% humidity	(13)
MHV	*Betacoronavirus*	*Embecovirus*	MHV-2	Cellular infectivity in DBT cells (PFU)	40[b], 60, 80[a]	MEM containing 2% FCS	(50)
MHV	*Betacoronavirus*	*Embecovirus*	MHV-N	Cellular infectivity in DBT cells (PFU)	40[b], 60, 80[a]	MEM containing 2% FCS	(50)
MHV	*Betacoronavirus*	*Embecovirus*	A59	Plaque assay on L2 cells	10[b], 25	Pasteurized wastewater	(57)
PEDV	*Alphacoronavirus*	*Pedacovirus*	V215/78	PFU on Vero cells	50	Diluted medium for virus replication	(58)
PEDV	*Alphacoronavirus*	*Pedacovirus*	CV777	Vero cells (TCID-50)	40, 44, 48	MEM at pH 7.2	(59)
PEDV	*Alphacoronavirus*	*Pedacovirus*	CV777	Vero cells (TCID-50)	4[b], 44[b], 48	Medium at pH 7.5	(60)
SARS-CoV	*Betacoronavirus*	*Sarbecovirus*	FFM-1	Cellular infectivity in Vero cells	56	Cell culture supernatant with or without FBS	(20)
SARS-CoV	*Betacoronavirus*	*Sarbecovirus*	Urbani	Cellular infectivity in Vero cells	56, 65, and 75[a]	Dulbecco's MEM	(61)
SARS-CoV	*Betacoronavirus*	*Sarbecovirus*	HKU39849	Cellular infectivity in FRH-K4 (TCID-50)	28, 33, 38	Plastic stored at 95% RH	(62)
SARS-CoV	*Betacoronavirus*	*Sarbecovirus*	HKU39849	Cellular infectivity in FRH-K4 (TCID-50)	28[b], 33, 38	Plastic stored at 80-89% RH	(62)
SARS-CoV	*Betacoronavirus*	*Sarbecovirus*	GVU6109	Cellular infectivity in Vero cells (TCID-50)	20	Viral Transport Medium(VTM)	(43)
SARS-CoV	*Betacoronavirus*	*Sarbecovirus*	GVU6109	Cellular infectivity in Vero cells (TCID-50)	4, 20	Nasopharyngeal aspirate (NPA), throat and nasal swab (TNS)	(43)

						or VTM	
SARS-CoV	*Betacoronavirus*	*Sarbecovirus*	Tor2 AY274119.3	Cellular infectivity in Vero cells (TCID-50)	22	Plastic and stainless steel stored at 40°C	(12)
SARS-CoV	*Betacoronavirus*	*Sarbecovirus*	Utah	Cellular infectivity in Vero cells (TCID-50)	58, 68	Iscove's 4% FCS medium	(63)
SARS-CoV	*Betacoronavirus*	*Sarbecovirus*	Utah	Cellular infectivity in Vero cells (TCID-50)	22	Glass surface store at 10-25% RH	(63)
SARS-CoV	*Betacoronavirus*	*Sarbecovirus*	Hanoi	Cellular infectivity in Vero cells (TCID-50)	56	MEM	(64)
SARS-CoV2	*Betacoronavirus*	*Sarbecovirus*	-	Cellular infectivity in Vero cells (TCID-50)	4, 22, 37, 56, 70 [a]	VTM	(11)
SARS-CoV2	*Betacoronavirus*	*Sarbecovirus*	-	Cellular infectivity in Vero cells (TCID-50)	22	Plastic and stainless steel at 65% RH	(11)
SARS-CoV2	*Betacoronavirus*	*Sarbecovirus*	WA1-2020 (MN985325.1)	Cellular infectivity in Vero cells (TCID-50)	22	Plastic and stainless steel stored at 40°C	(12)
SARS-CoV2	*Betacoronavirus*	*Sarbecovirus*	-	Cellular infectivity in Vero cells (TCID-50)	56, 65[a]	Cell culture supernatants	(65)
SARS-CoV2	*Betacoronavirus*	*Sarbecovirus*	-	Cellular infectivity in Vero cells (TCID-50)	65, 95[a]	Nasopharyngal samples	(65)
SARS-CoV2	*Betacoronavirus*	*Sarbecovirus*	-	Cellular infectivity in Vero cells (TCID-50)	56	Sera	(65)
TGEV	*Alphacoronavirus*	*Tegacovirus.*	D52	Cellular infectivity in RPtg cells	31, 35, 39, 43, 47, 51 and 55	In HEPES solution at pH 7	(16)
TGEV	*Alphacoronavirus*	*Tegacovirus.*	D52	Cellular infectivity in RPtg cells	35, 39, 43, 47, and 51	In HEPES solution at pH 8	(16)
TGEV	*Alphacoronavirus*	*Tegacovirus.*	-	Cellular infectivity in ST cells	4[b], 20, 40	Stainless steel surface with 20% RH	(13)
TGEV	*Alphacoronavirus*	*Tegacovirus.*	-	Cellular infectivity in ST cells	4, 20, 40	Stainless steel surface with 50% RH	(13)
TGEV	*Alphacoronavirus*	*Tegacovirus.*	-	Cellular infectivity in ST cells	4, 20, 40	Stainless steel surface with 80% RH	(13)
TGEV	*Alphacoronavirus*	*Tegacovirus.*	-	Cellular infectivity in ST cells	4[b], 25	Reagent-grade water	(39)
TGEV	*Alphacoronavirus*	*Tegacovirus.*	-	Cellular infectivity in ST cells	4[b], 25	Lake water	(39)

[a] not included: limit of quantification reached for the first sample time
[b] not included: not enough decrease observed during experimentation
- data not specified

507 **Table 2. Characteristics of the different models fitted to the 102 decimal reduction time**

508 **data of coronaviruses according to temperature (T_{ref} set at 4°C) and relative humidity**

Model	Fitted parameters	Best fit values [95%CI bootstrap intervals]	Bayesian information criterion	Aikaike information criterion
Model #1	log10Dref	3.1 [2.8 - 3.3]	-124.7	-130.0
	z_T	13.8 [12.7 - 15.1]		
Model #2	log10Dref	2.2 [2.1 - 2.3]	-160.6	-165.9
	z_T	29.4 [28.4 - 30.5]		
Model #3	log10Dref	2.3 [2.1 - 2.6]	-156.7	-164.6
	z_T	27.7 [23.2 – 31.6]		
	n	1.9 [1.5 - 2.2]		
Model #4	log10Dref	2.3 [2.2 - 2.5]	-160.2	-168.0
	z_T	29.1 [28.1 - 30.1]		
	z_{RH}	341.4.7 [190.1 - 5631.4]		
Model #5	log10Dref	2.4 [2.2 - 2.6]	-156.2	-166.6
	z_T	27.5 [23.6 - 31.2]		
	z_{RH}	330.7 [182.8 – 7020,1]		
	n	1.9 [1.6 - 2.2]		

509

510

Figure 1. Decimal reduction times of ten coronaviruses according to temperature in suspension or on inert surfaces.

Figure 2. Observed (points) and fitted (grey lines) log decimal reduction time values according to temperature for model #1 (A), model #2 (B) and #3 (C). One thousand (1000) bootstrap values of uncertainty characterization are shown. Estimates of model parameters are given in Table 2.

Figure 3. (A) Observed inactivation rate values (grey points) according to temperature (°C) and relative humidity (%) and Model #4 surface predictions. Scatter points of observed versus predicted D-values (D in hours) for model #4 (B). The dashed line represents a perfect match between observations and predictions.

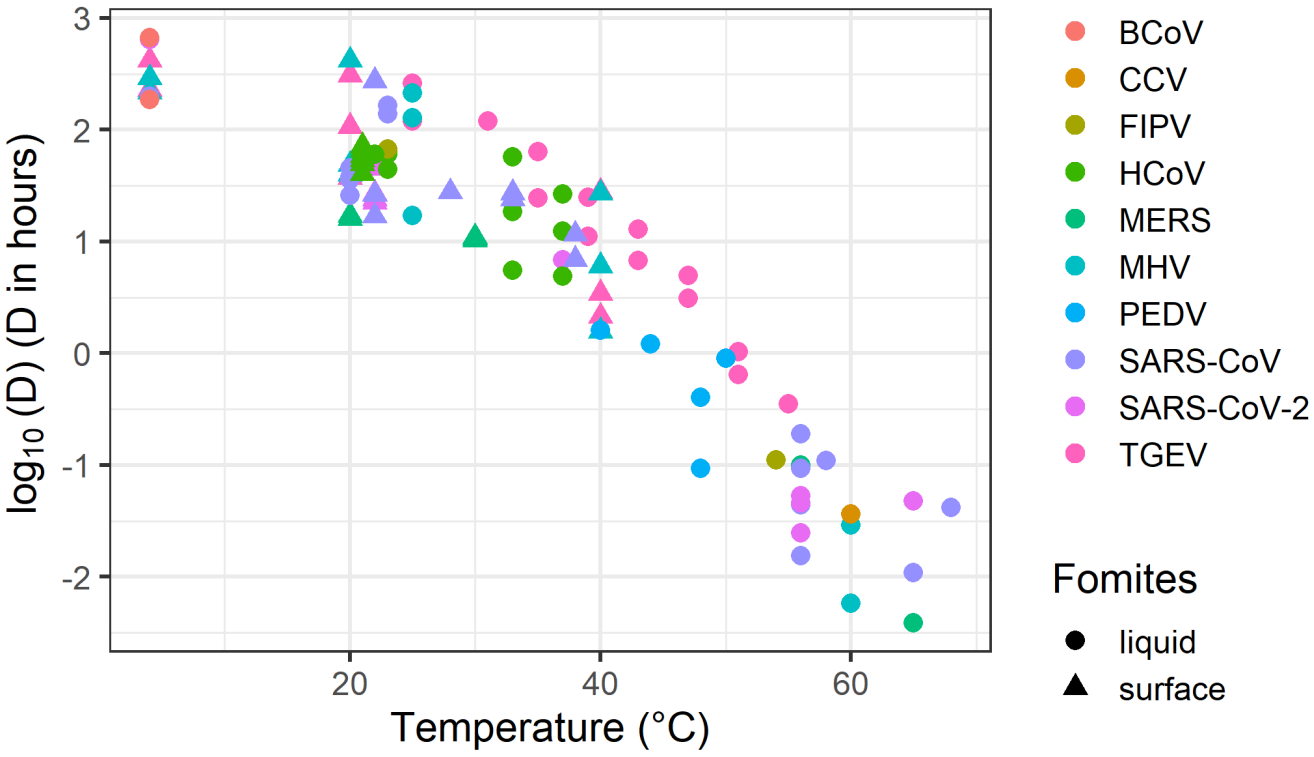
3
2
1
0
-1
-2
log10 (D) (D in hours)
20
40
60
Temperature (°C)
BCoV
CCV
FIPV
HCoV
MERS
MHV
PEDV
SARS-CoV
SARS-CoV-2
TGEV
Fomites
liquid
surface

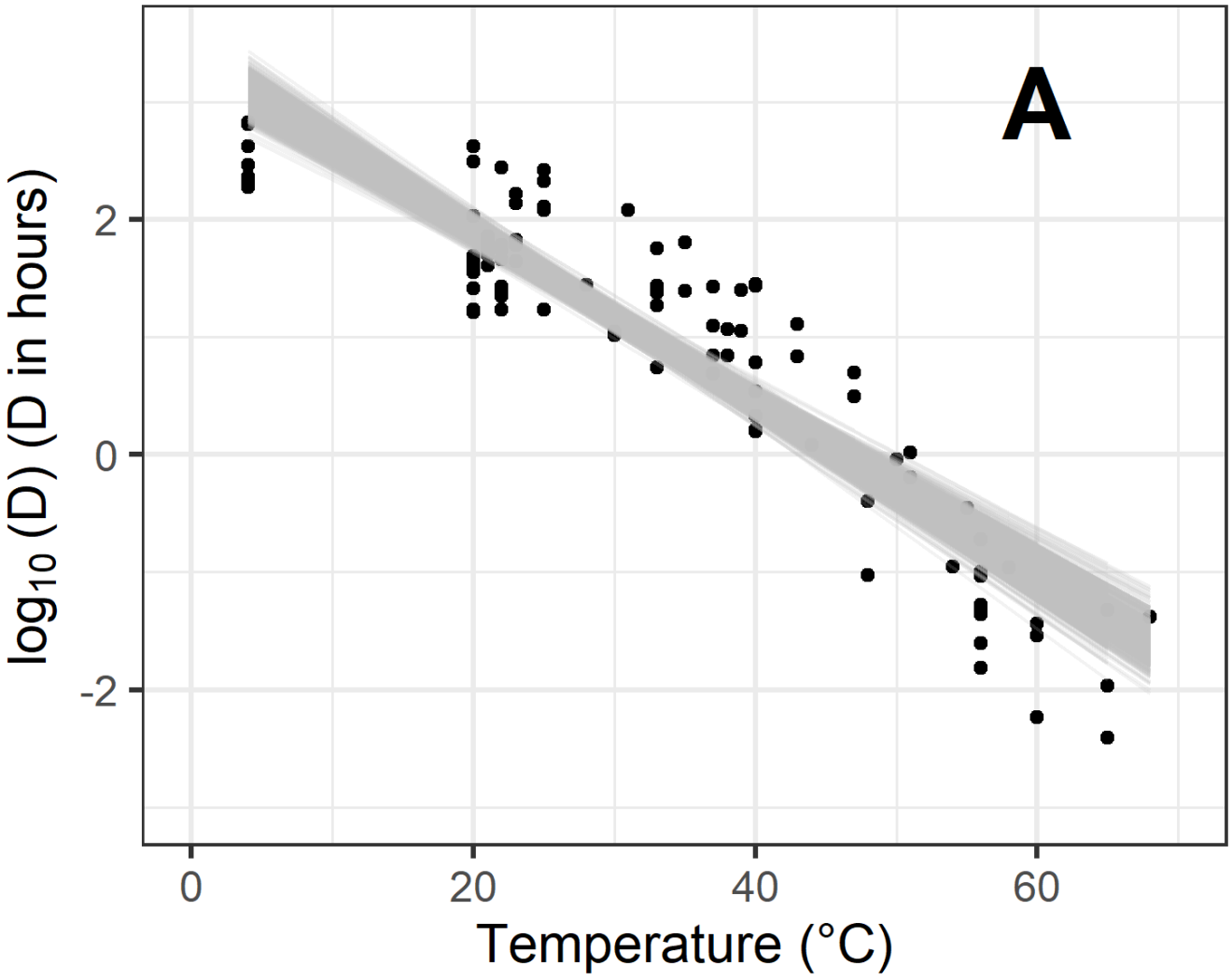
A
log10 (D) (D in hours)
2
0
-2
0
20
40
60
Temperature (°C)

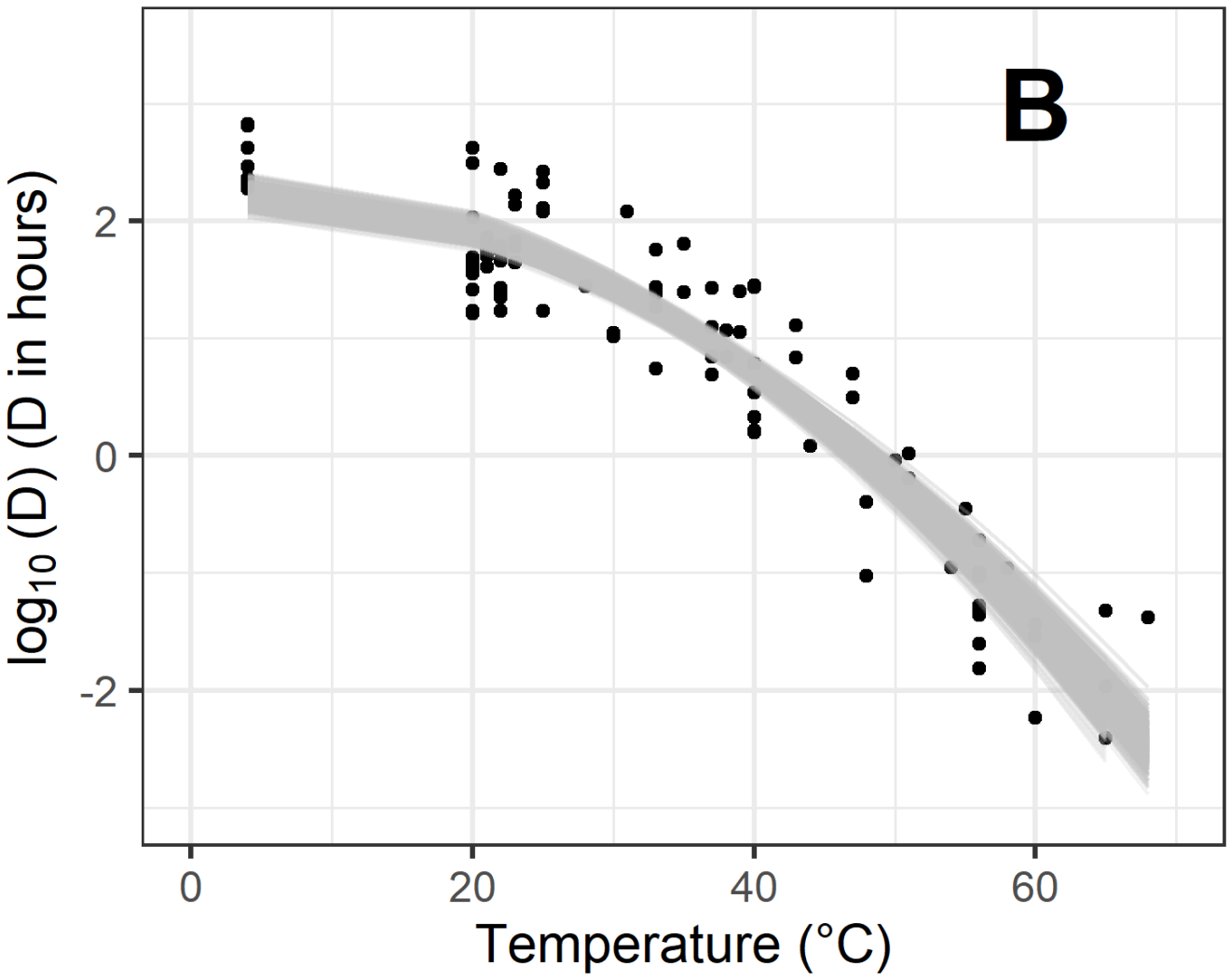
B
log10 (D) (D in hours)
2
0
-2
0
20
40
60
Temperature (°C)

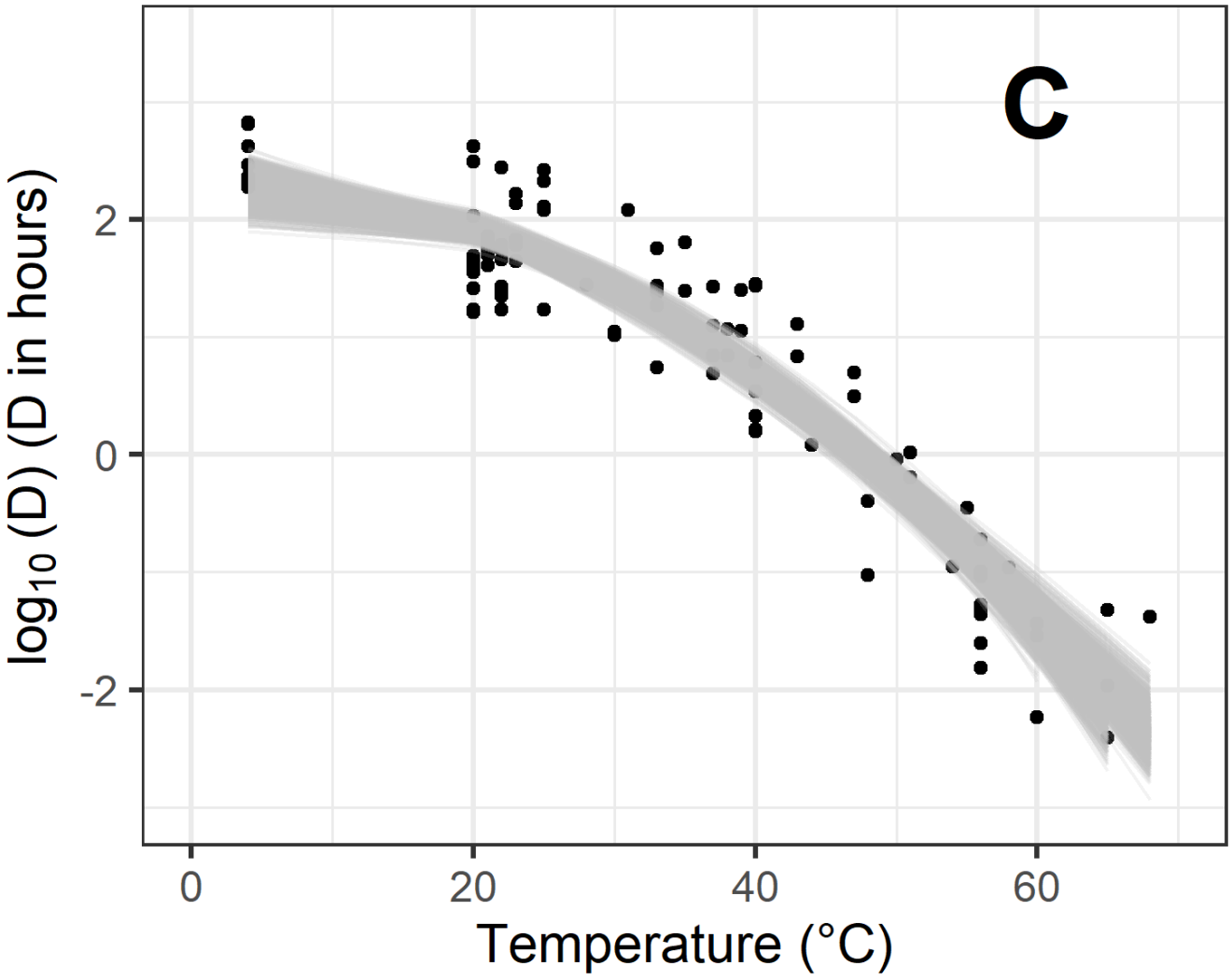
C
log10 (D) (D in hours)
2
0
-2
0
20
40
60
Temperature (°C)

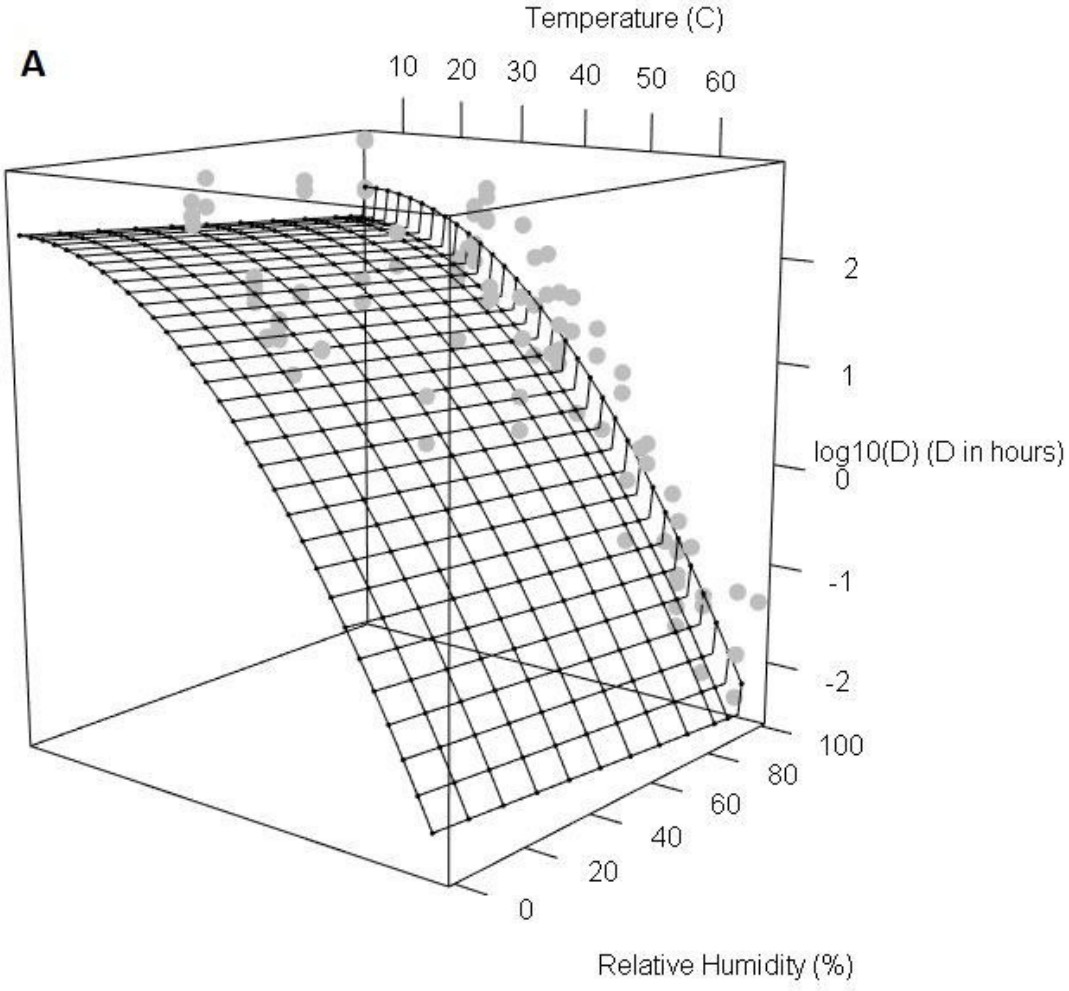
A
Temperature (C)
10
20
30
40
50
60
2
1
log10(D) (D in hours)
0
-1
-2
100
80
60
40
20
0
Relative Humidity (%)

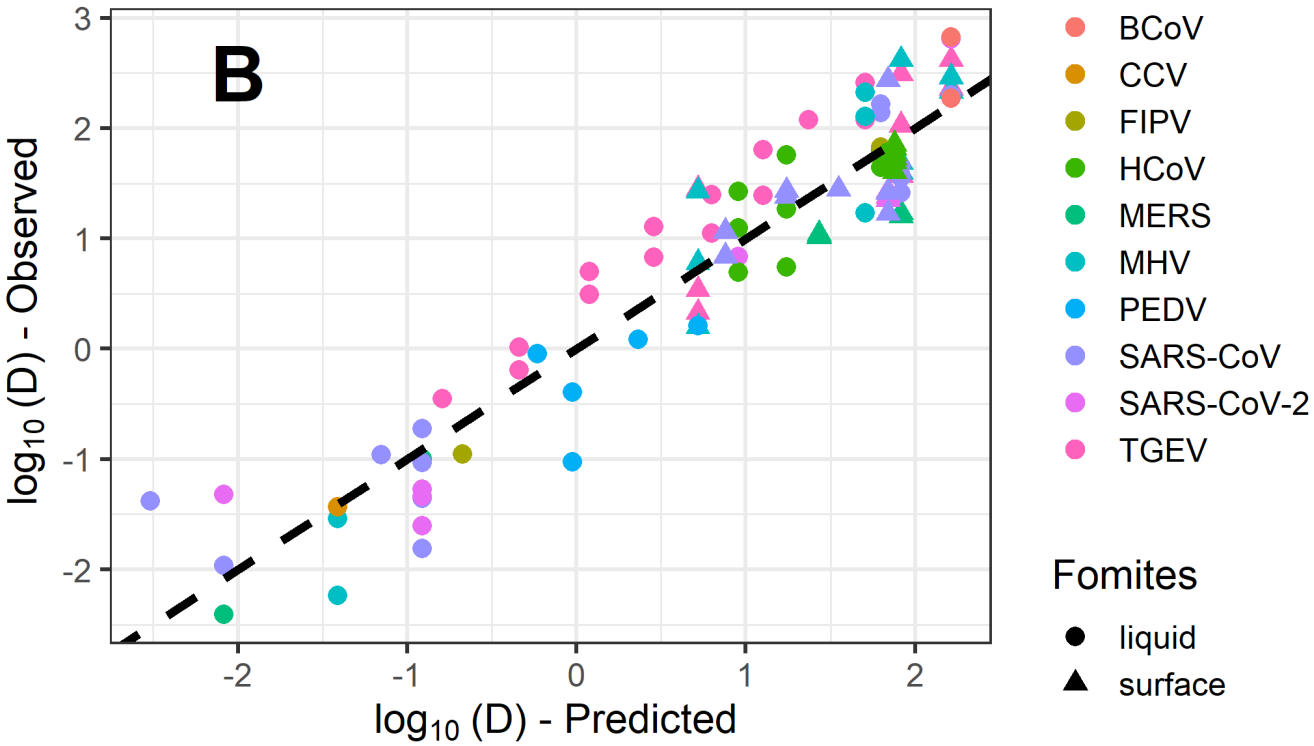
B
log10 (D) - Observed
log10 (D) - Predicted
3
2
1
0
-1
-2
-2
-1
0
1
2
BCoV
CCV
FIPV
HCoV
MERS
MHV
PEDV
SARS-CoV
SARS-CoV-2
TGEV
Fomites
liquid
surface